



NEURO



Quantitative T_1 brain mapping in early relapsing-remitting multiple sclerosis: longitudinal changes, lesion heterogeneity and disability

James G. Harper¹ , Elizabeth N. York^{1,2,3*} , Rozanna Meijboom^{1,2}, Agniete Kampaite^{1,2}, Michael J. Thrippleton^{1,2}, Patrick K. A. Kearns^{1,3}, Maria del C. Valdés Hernández^{1,2}, Siddharthan Chandran^{1,3,4} and Adam D. Waldman^{1,2*} on behalf of On behalf of the FutureMS consortium

Abstract

Objectives To quantify brain microstructural changes in recently diagnosed relapsing-remitting multiple sclerosis (RRMS) using longitudinal T_1 measures, and determine their associations with clinical disability.

Methods Seventy-nine people with recently diagnosed (<6 months) RRMS were recruited from a single-centre cohort sub-study, and underwent baseline and 1-year brain MRI, including variable flip angle T_1 mapping. Median T_1 was measured in white matter lesions (WML), normal-appearing white matter (NAWM), cortical/deep grey matter (GM), thalami, basal ganglia and medial temporal regions. Prolonged T_1 (≥ 2.00 s) and supramedian T_1 (relative to cohort WML values) WML voxel counts were also measured. Longitudinal change was assessed with paired t -tests and compared with Bland-Altman limits of agreement from healthy control test-retest data. Regression analyses determined relationships with Expanded Disability Status Scale (EDSS) score and dichotomised EDSS outcomes (worsening or stable/improving).

Results Sixty-two people with RRMS (mean age 37.2 ± 10.9 [standard deviation], 48 female) and 11 healthy controls (age 44 ± 11 , 7 female) contributed data. Prolonged and supramedian T_1 WML components increased longitudinally (176 and 463 voxels, respectively; $p < .001$), and were associated with EDSS score at baseline ($p < .05$) and follow-up (supramedian: $p < .01$; prolonged: $p < .05$). No cohort-wide median T_1 changes were found; however, increasing T_1 in WML, NAWM, cortical/deep GM, basal ganglia and thalami was positively associated with EDSS worsening ($p < .05$).

Conclusion T_1 is sensitive to brain microstructure changes in early RRMS. Prolonged WML T_1 components and subtle changes in NAWM and GM structures are associated with disability.

Clinical relevance statement MRI T_1 brain mapping quantifies disability-associated white matter lesion heterogeneity and subtle microstructural damage in normal-appearing brain parenchyma in recently diagnosed RRMS, and shows promise for early objective disease characterisation and stratification.

James G. Harper and Elizabeth N. York contributed equally to this work and are joint first authors.

*Correspondence:

Elizabeth N. York

eyork@ed.ac.uk

Adam D. Waldman

adam.waldman@ed.ac.uk

Full list of author information is available at the end of the article

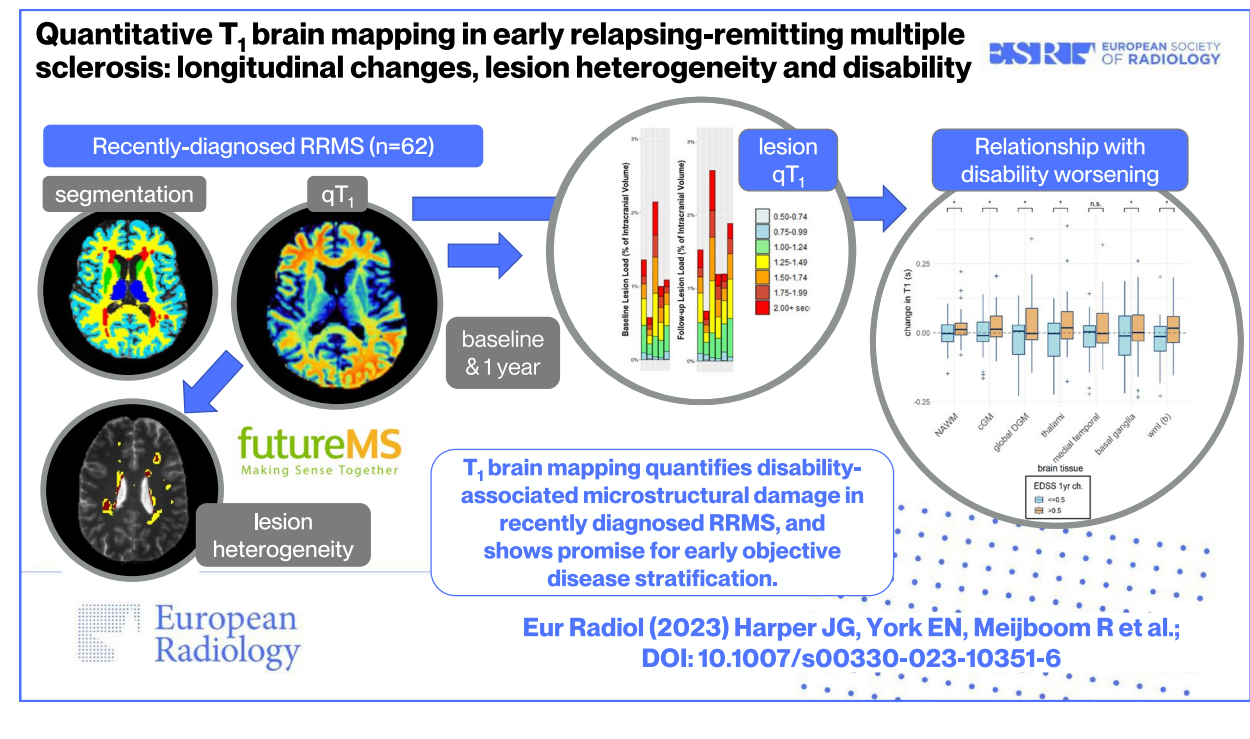


© The Author(s) 2023. **Open Access** This article is licensed under a Creative Commons Attribution 4.0 International License, which permits use, sharing, adaptation, distribution and reproduction in any medium or format, as long as you give appropriate credit to the original author(s) and the source, provide a link to the Creative Commons licence, and indicate if changes were made. The images or other third party material in this article are included in the article's Creative Commons licence, unless indicated otherwise in a credit line to the material. If material is not included in the article's Creative Commons licence and your intended use is not permitted by statutory regulation or exceeds the permitted use, you will need to obtain permission directly from the copyright holder. To view a copy of this licence, visit <http://creativecommons.org/licenses/by/4.0/>.

Key Points

- Quantitative T_1 mapping detects brain microstructural damage and lesion heterogeneity in recently diagnosed relapsing-remitting multiple sclerosis.
- T_1 increases in lesions and normal-appearing parenchyma, indicating microstructural damage, are associated with worsening disability.
- Brain T_1 measures are objective markers of disability-relevant pathology in early multiple sclerosis.

Keywords Magnetic resonance imaging, Multiple sclerosis (Relapsing-Remitting), Longitudinal studies, Brain, Multiparametric magnetic resonance imaging

Graphical abstract**Introduction**

Disease trajectory in relapsing-remitting multiple sclerosis (RRMS) is highly variable, and difficult to predict early in the disease course. Improved objective prognostic markers, which are sensitive to early RRMS pathological features, are needed to better inform early treatment decisions from the point of diagnosis, and for future clinical trials.

Episodic immune-mediated demyelination is thought to result in axonal damage and neuronal dysfunction [1]. Identification of new or enlarging white matter lesions (WML) visible on T_2 -weighted or T_2 -FLAIR (fluid-attenuated inversion recovery) MRI is widely used as an indicator of interval inflammatory disease activity [2]. The number and volume of WML do not, however, adequately explain clinical disability in RRMS [3, 4]. Microscopic damages

to grey matter (GM) and normal-appearing white matter (NAWM) are also pathological features of RRMS, [5] and heterogeneity of microstructural damage within WML that appears similar on T_2 -weighted MRI is observable using quantitative microstructure-sensitive MRI methods [6–9].

A subset of T_2 -weighted WML are visibly hypointense on T_1 -weighted MRI, reflecting T_1 prolongation, [10] and have variously been described as ‘black hole’ or ‘ T_1 w-hypointense’ lesions [11]. Such ‘ T_1 w-hypointense’ lesions are thought to represent more severely damaged white matter [12] and are associated with worse clinical disability [13, 14]. Radiological evaluation of T_1 -weighted hypointensity is nevertheless subjective and qualitative, and will not capture intralesional T_1 heterogeneity or subtle change in normal-appearing tissue.

The spin-lattice relaxation time (T_1) of protons in brain parenchyma is inversely proportional to myelin density [11]. Previous imaging-histological correlation indicates that T_1 quantification may provide a non-invasive marker of myelin density in multiple sclerosis (MS), [12] and is sensitive to subtle abnormalities in normal-appearing GM and NAWM in RRMS [5, 15–20]. Widespread T_1 prolongation is seen in RRMS compared with healthy controls, and correlates with disability [14, 20, 21]. Quantitative mapping of T_1 may also distinguish microstructural heterogeneity within WML; substantially prolonged T_1 tissue volumes appear to be a better predictor of disability than visual assessment of T_1 -weighted hypointense WML [22]. The contribution of prolonged T_1 components in WML and other brain tissues to clinical disability in early disease, and how these evolve with time remain to be explored.

The primary aims of this study were to assess whether changes in tissue microstructure integrity, reflected in T_1 heterogeneity and prolongation, are quantifiable within WML and other brain regions over the first year following RRMS diagnosis, and to ascertain the relationship between T_1 prolongation and clinical disability. We

hypothesised that prolonged T_1 components would progress with time and be associated with worsening clinical disability.

Our secondary exploratory aims were to examine intralésional T_1 heterogeneity and its relationship with disability, investigate single-time point measures as predictors of clinical disability trajectory following RRMS diagnosis and establish the test-retest reliability of T_1 measures.

Materials and methods

Ethics approval was obtained from the South East Scotland Research Ethics Committee 02 (REC 15/SS/0233). The study conformed to the Declaration of Helsinki 2000 (amendments in 2002 and 2004) and Good Clinical Practice ICH guidelines. All participants gave written informed consent and data were pseudo-anonymised.

Participants

Seventy-nine patients were recruited to a single-centre sub-study of FutureMS, a prospective multi-centre longitudinal inception cohort study of people with recently diagnosed RRMS across Scotland (Fig. 1) [23, 24]. Inclusion criteria were as follows: < 6 months from

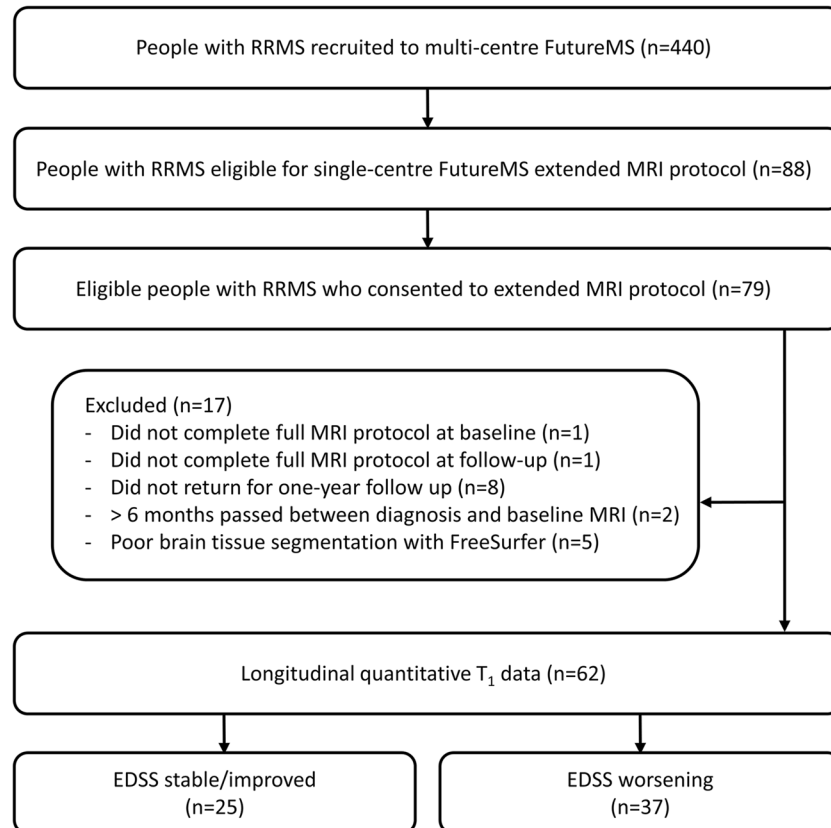


Fig. 1 Flowchart showing inclusion and exclusion criteria for FutureMS quantitative T_1 sub-study

diagnosis; aged ≥ 18 years; and capacity to provide informed consent. Exclusion criteria were as follows: previous use of disease-modifying therapies (DMTs); clinical trial participation prior to baseline assessment; and contraindications for MRI. FutureMS sample size calculation has been previously described; [24] Edinburgh participants were pragmatically offered extended MRI once the sub-study recruitment opened in November 2017 until March 2019. Twelve age- and sex-matched healthy controls were recruited for test-retest purposes. Exclusion criteria were contraindication for MRI and incidental MRI findings.

MRI and Expanded Disability Status Scale (EDSS) score were acquired at baseline (between November 2017 and July 2019) and 1-year follow-up. Handling of missing data and loss to follow-up are detailed elsewhere; briefly, data missing at random were imputed using predictive mean matching [23].

MRI protocol

MRI was performed on a 3-Tesla Siemens MAGNETOM Prisma clinical system at the University of Edinburgh Imaging Facility. Whole-brain T_1 mapping

was performed using a variable flip angle (VFA) 3D multi-echo spoiled gradient recalled echo sequence (total acquisition time: 12 min 28 s) as part of a comprehensive MRI protocol, including a 2D T_2 -weighted FLAIR and 3D T_1 -weighted MPRAGE (Table S1) [24]. Control subjects underwent an identical MRI protocol, repeated within 2 weeks, to determine test-retest agreement.

Structural MRI data processing

WML segmentation was performed on baseline 2D T_2 FLAIR images using an adaptation of a previously reported thresholding method, [25] with manual correction [24]. Tissues were segmented with FreeSurfer (v6.0, <http://surfer.nmr.mgh.harvard.edu/>) from the T_1 -weighted MPRAGE [24]. These included NAWM; cortical GM (cGM); medial temporal regions (hippocampi and amygdala); basal ganglia (caudate, pallidum and putamen); thalami; and global deep GM (DGM; combined thalami, basal ganglia and medial temporal regions; Fig. 2). WML load was calculated as the percentage of occupied intracranial volume [24].

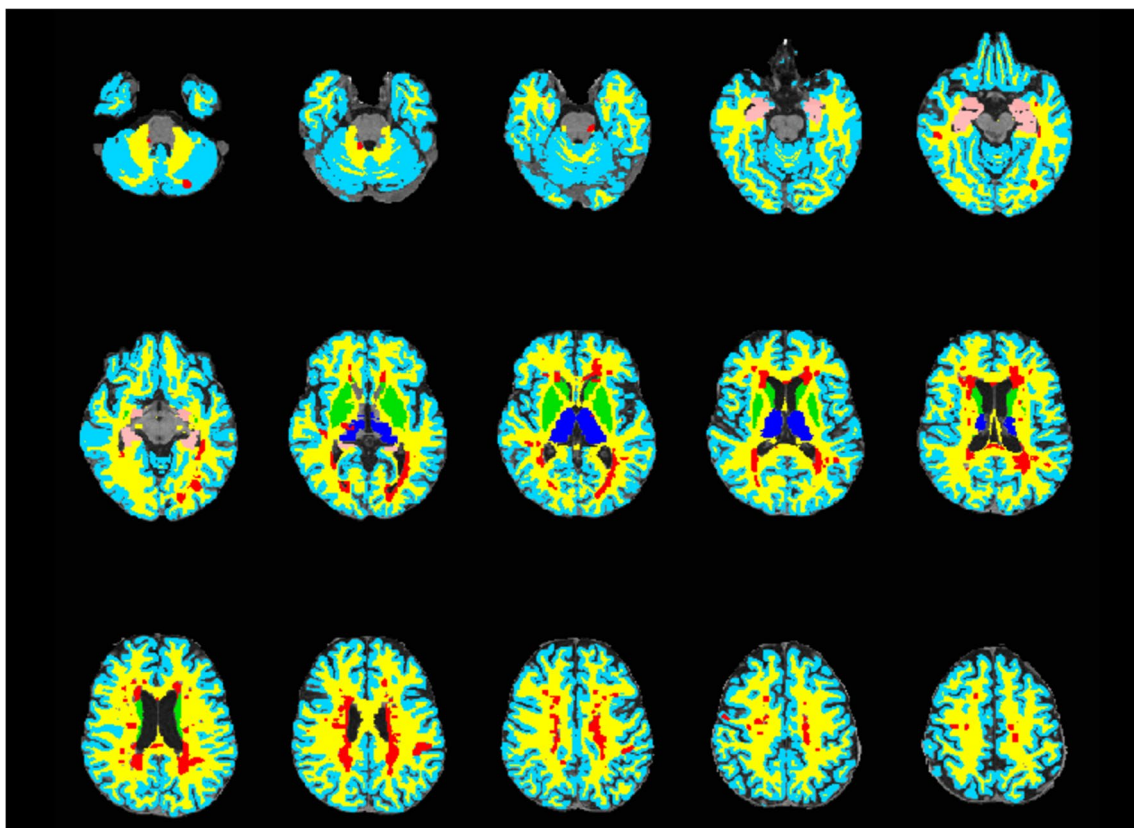


Fig. 2 An axial T_1 map with superimposed brain tissue segmentations: normal-appearing white matter (yellow), white matter lesions (red), cortical grey matter (light blue), thalami (dark blue), basal ganglia (green) and medial temporal regions (pink)

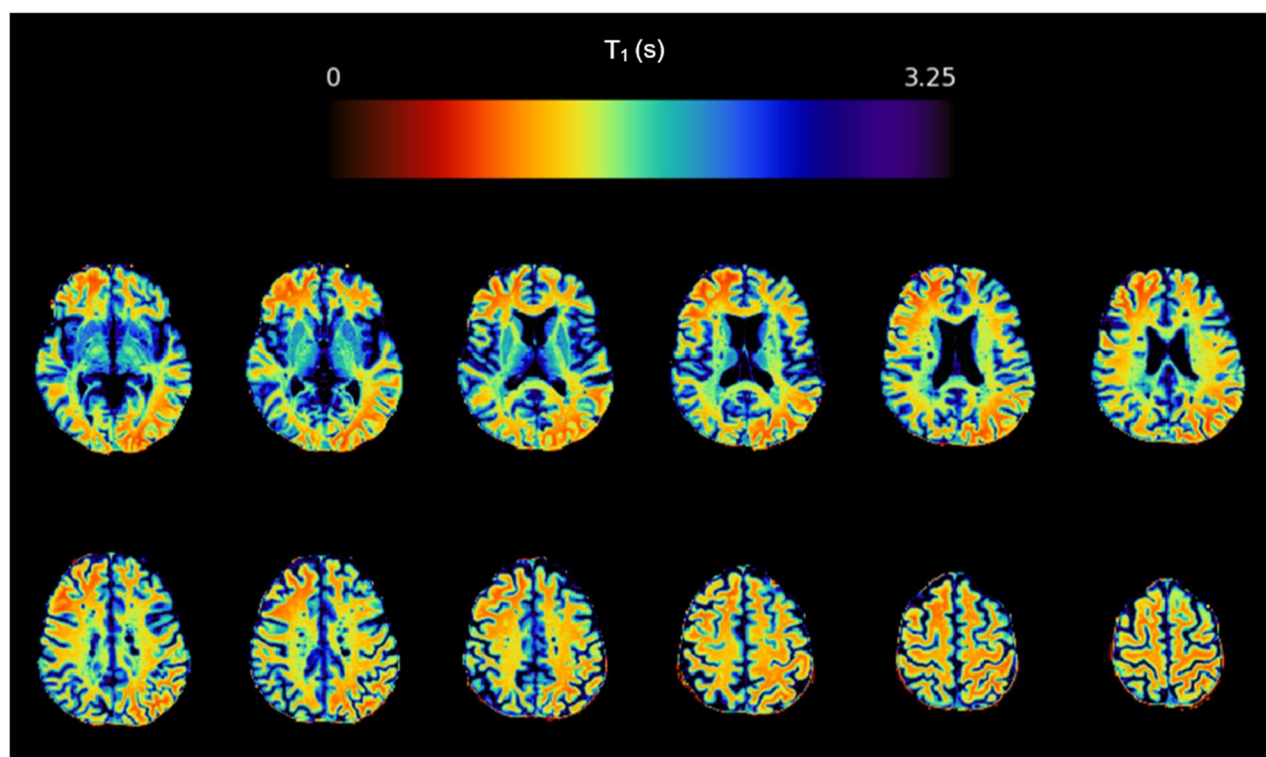


Fig. 3 Axial T_1 (colour) map brain slices for a person with recently diagnosed relapsing-remitting multiple sclerosis taking part in FutureMS. The colour bar represents T_1 in seconds of the colour scale

T_1 data processing

T_1 parametric maps were obtained from VFA gradient echo images in MATLAB (R2018b) using previously described equations (Fig. 3; software available: <https://doi.org/10.7488/ds/2965>) [26, 27]. Tissue segmentations were registered to T_1 maps using FSL (v6.0.1) FLIRT [28].

Median T_1 within each tissue was calculated per patient (fslstats). To investigate T_1 WML heterogeneity, the proportion of WML voxels within each 0.25-s interval between 0.5 and 2.00 s was calculated for each patient at baseline and follow-up (RStudio v4.0.2).

As T_1 prolongation is associated with demyelination [12] and disability, [3] we also characterised WML components with relatively prolonged T_1 using a thresholding approach [22]. The number of WML voxels with (1) $T_1 \geq 2.00$ s (here termed ‘prolonged T_1 ’) and (2) supramedian T_1 (calculated per patient relative to the baseline cohort mean of WML median T_1) was thus calculated at each time point.

Statistical analysis

All statistical analyses were performed in RStudio (v4.0.2).

Test-retest healthy controls

To establish test-retest reference levels, Bland-Altman limits of agreement were calculated from healthy control

data, following previously reported methodology [29]. To assess whether the difference between time points was statistically significant, sign tests were performed.

Longitudinal change in T_1 metrics

Paired two-sided *t*-tests were used to examine longitudinal changes in median T_1 for each tissue and, as separate analyses, 1-year changes in the number of prolonged/supramedian T_1 voxels and WML load. To account for WML voxels forming during the 1-year follow-up period, which could positively skew WML T_1 data, a post hoc paired *t*-test was performed including only WML voxels already present at baseline. T_1 changes in NAWM and cGM were plotted against test-retest limits for visual comparison. To control for type II error, False Discovery Rate (FDR) correction ($q < 0.05$) was applied for primary analyses [30].

Relationship with clinical disability

The relationship between T_1 and EDSS score at baseline was investigated using ordinal logistic regression. In view of limited EDSS changes within our recently diagnosed cohort, 1-year change in EDSS score was dichotomised as either worsening EDSS, defined as ≥ 0.5 points, or stable/improving; the relationship between disability groups and both baseline and 1-year changes in T_1 measures was

Table 1 Cohort demographics of the relapsing-remitting multiple sclerosis (RRMS) participants. Differences between disability groups were assessed with Welch's *t*-test for age, baseline/follow-up Expanded Disability Status Scale (EDSS) score, white matter lesion load and interval between baseline and follow-up MRI, and Pearson's chi-squared (X^2) test of independence with Yates' continuity correction for sex and disease-modifying therapy (DMT) status

	Cohort	Stable/improving EDSS	Worsening EDSS
Number of RRMS participants	62	25	37
Mean age (SD) [range] in years	37.2 (10.9) [21 to 67]	36.7 (9.7) [22 to 59]	37.5 (11.9) [21 to 67]
Sex (female:male)	48:14	19:6	29:8
Median baseline EDSS score [range]	2 [0 to 6]	2 [0 to 3.5]	2 [0 to 6]
Median follow-up EDSS score [range]	2.5 [0 to 6.5]	2 *** [0 to 3.5]	3 *** [1.5 to 6.5]
Number of participants on disease-modifying therapies at 1-year follow-up	38 (61%)	17 (68%)	21 (57%)
Mean interval (SD) [range] between baseline and 1-year MRI in days	385 (35.2) [339 to 520]	383 (28.9) [339 to 451]	386 (39.2) [352 to 520]
Mean baseline lesion load (%ICV)	0.802	0.570	0.959
Mean change in lesion load	0.235	0.196	0.261

Asterisks mark significant differences: * < 0.05, *** < 0.001

RRMS, relapsing-remitting multiple sclerosis; EDSS, Expanded Disability Status Scale; SD, standard deviation; ICV, intracranial volume

investigated using binomial logistic regression, adjusted for covariates and interactions as appropriate (Table S2 for extended methods). FDR correction was applied separately for the three sets of analyses, which are assumed to be distinct families of hypotheses [30].

Regression analyses were repeated for prolonged and supramedian T_1 WML measures. The relationship between WML prolonged T_1 measures at 1-year follow-up and EDSS score at follow-up was also investigated using ordinal logistic regression.

Results

Demographics

Complete data were available from sixty-two RRMS patients (Fig. 1), and demographics (Table 1) were comparable to the wider FutureMS cohort [23]. Six participants ($n=3$ worsening versus $n=3$ stable/improving disability) reported a relapse in the 6 weeks prior to baseline MRI (range: 11–34 days), one of whom received oral steroid treatment (27 days before MRI). No relapses or steroid treatments were reported in the 6 weeks prior to follow-up. At follow-up, 61% ($n=38$) of participants had begun treatment with DMTs, mainly dimethyl fumarate ($n=23$; Table S3). There was no significant difference in DMT status between disability groups ($X^2=0.79$, $p=0.37$).

One control participant was excluded due to an unexpected incidental finding; test–retest data was therefore available from eleven controls (age 44 ± 11 , 7 female).

Test-retest reliability

Test-retest agreement determined from control data is shown in Fig. S1. The difference in median T_1 was not significant for all brain regions (Table S4).

Characterising T_1 in white matter lesions

Qualitative assessment showed varied proportions of WML voxels within each 0.25-s T_1 range between patients, with a greater proportion in higher T_1 ranges at follow-up (Fig. 4b) relative to baseline (Fig. 4a). Visual inspection showed discrete regions of relative T_1 prolongation were present across WML (Fig. 5a–c), generally coinciding with T_1 -weighted 'black holes' (Fig. 5d–f).

Longitudinal change in T_1 metrics

WML median T_1 decreased by a mean average of 31 ms longitudinally ($t(61)=2.98$, FDR-corrected $p<0.05$, 95% CI $[-52, -10]$); no other tissues showed significant longitudinal T_1 changes (Table 2). Longitudinal change in NAWM and WML T_1 for the majority of patient data points fell within test–retest Bland-Altman limits established in healthy controls (Fig. S2).

A longitudinal increase in WML load (mean average 0.235%, $t(61)=11.3$, $p<0.001$, 95% CI $[0.193, 0.277]$) prompted a post hoc analysis investigating only WML voxels present at baseline. This showed no significant change in median WML T_1 ($t(61)=0.50$, $p=0.618$; Table 2).

There was a groupwise mean increase of 176 prolonged T_1 WML voxels ($t(61)=5.11$, $p<0.001$, 95% CI $[107, 246]$) and an increase of 463 supramedian WML voxels ($t(61)=6.22$, $p<0.001$, 95% CI $[314, 612]$). When WML voxels which had formed during the follow-up period were excluded, changes in both measures remained significant ($p<0.001$).

Relationship with clinical disability

Baseline median T_1 was not associated with baseline EDSS score (all $p>0.05$; Table S5) nor with EDSS

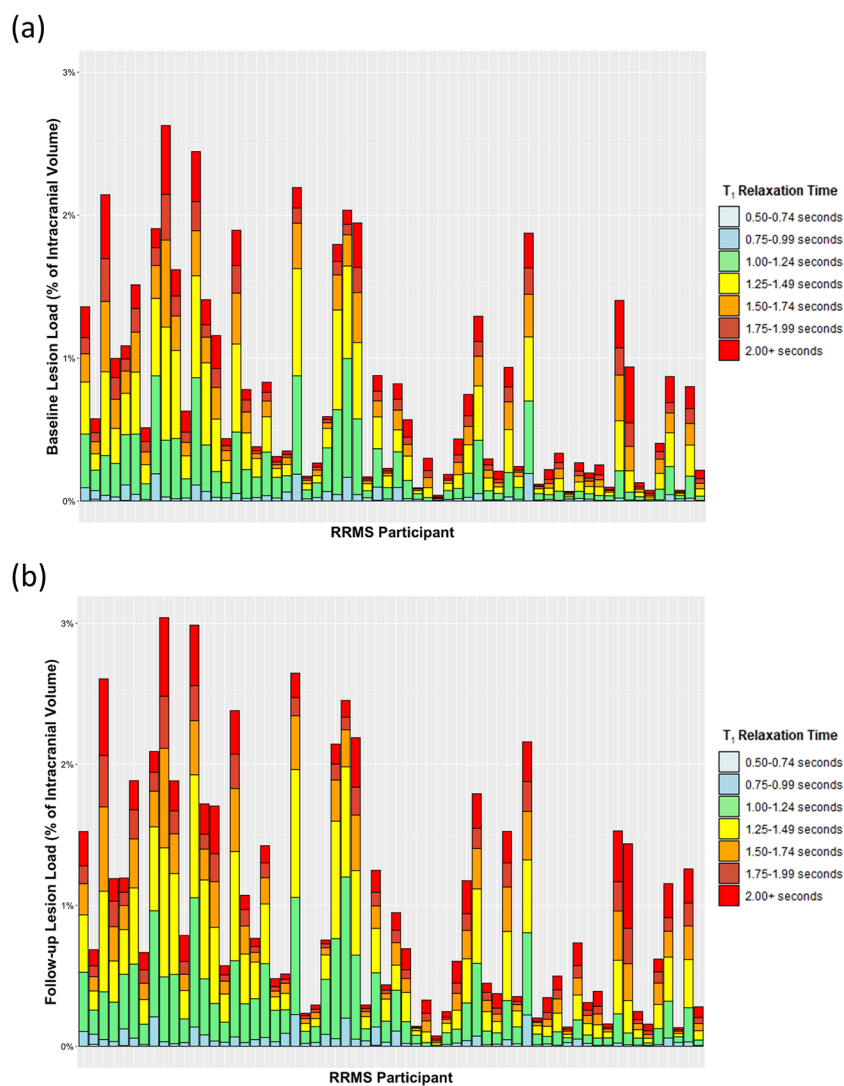


Fig. 4 White matter lesion T_1 heterogeneity in our cohort of people with recently diagnosed relapsing-remitting multiple sclerosis (RRMS) ($n=62$). Each bar represents one participant with RRMS. The colours of the stacked plot relate to the proportion of a given participant's white matter lesion voxels within a given T_1 range at (a) baseline and (b) 1-year follow-up

worsening (all $p > 0.05$; Table S6) in any tissue studied. One-year changes in T_1 (Table S7) within NAWM, WML, cGM, DGM, the basal ganglia and thalami (but not the medial temporal regions) were however positively associated with a greater risk of EDSS worsening (all $p < 0.05$; Fig. 6, and Table 3). The relationship between change in WML T_1 and EDSS worsening was mediated by an interaction with age, whereby older age strengthened the association.

At baseline, greater numbers of prolonged T_1 and supramedian WML voxels were independently associated with higher baseline EDSS (both $p < 0.05$; Table 4); neither measure was predictive of EDSS worsening (Table 5). One-year changes in prolonged T_1 and

supramedian WML voxel counts were positively associated with EDSS worsening ($p < 0.05$ and $p < 0.01$ respectively; Table 5). Prolonged and supramedian WML T_1 measures at follow-up were also positively related with follow-up EDSS score ($p < 0.05$ and $p < 0.01$ respectively; Table 4).

Discussion

Brain T_1 , and its relationship with clinical worsening, was quantified longitudinally in a newly diagnosed RRMS cohort. Longitudinal cohort-wide changes in median T_1 were not observed for GM, NAWM or WML. There was significant T_1 heterogeneity in WML; WML voxels with

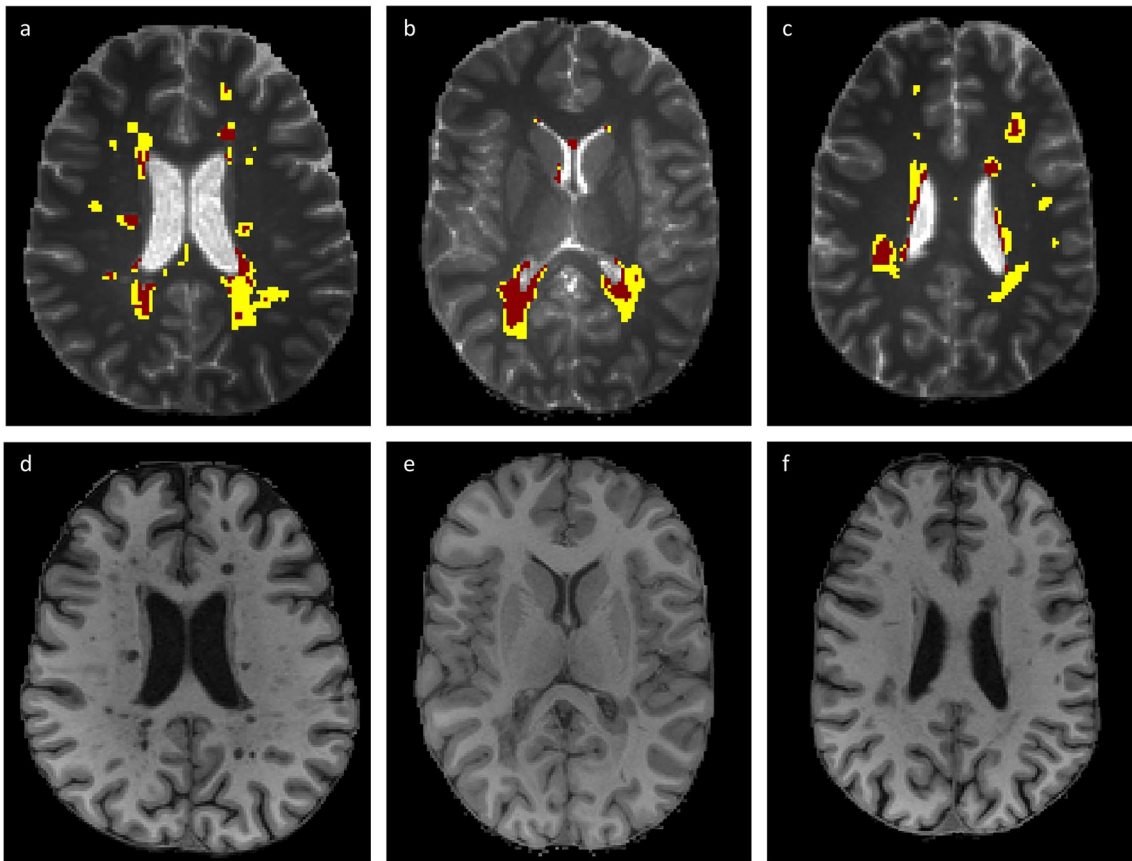


Fig. 5 Spatial distribution (a–c) of prolonged T_1 (i.e. ≥ 2.00 s) white matter lesion (WML) voxels (red) superimposed on all WML voxels (yellow) and whole-brain T_1 maps (greyscale) in three representative relapsing-remitting multiple sclerosis study participants, with corresponding T_1 -weighted MPRAGE structural images (d–f)

more marked T_1 prolongation increased in number over time, and were associated with disability at baseline and 1-year follow-up. Greater T_1 increases in normal-appearing brain and prolonged T_1 WML components also contributed significantly to evolving disability in the year following RRMS diagnosis.

T_1 variation

Measured T_1 was higher than literature values, [17, 22] which is attributable to differences in acquisition methods. Average WML T_1 values were higher than NAWM, consistent with demyelination [31]. As with previous findings in RRMS, [22] wide variance in WML T_1 and substantial overlap with cGM T_1 values suggest heterogeneous myelin loss; [12] in our cohort, average WML T_1 was lower than cGM, which may reflect the earlier disease stage and less severe WML damage. Medial temporal T_1 was significantly higher than other tissues; measurements in this region are likely confounded by tissue interface effects, and therefore unreliable.

Demyelination appears to be the major determinant of T_1 prolongation in white matter, [31] except within fully demyelinated WML where there is a ‘myelin floor effect’, and axonal content dominates variation in T_1 [12, 32]. Increased tissue water content, [11] due to neuroinflammation or oedema, [33, 34] may also increase T_1 . Subtle T_1 prolongation in NAWM is therefore likely to represent demyelination, whereas more markedly prolonged T_1 components within WML may result from both myelin and axonal loss. Myelin and axonal content are nonetheless strongly associated, [31] and we therefore use the term microstructural damage to reflect the difficulty in establishing their individual contributions to disability in WML and normal-appearing brain.

Our multiple threshold approach in WML is similar to methods applied previously, [22, 35] and analogous to histogram-based analyses [35, 36]. Our findings indicate varying degrees of microstructural damage across individuals at diagnosis, independent of WML load, which accords with lesion variation reported in more advanced disease across MS subtypes, [35, 37–39] and from other microstructure-sensitive methods [6–8].

Table 2 Brain tissue median T_1 summary statistics and results for paired t -tests

Brain tissue	T_1 (ms), mean \pm SD		Mean difference (ms) [95% CI]	t -value	p -value (uncorr.)	p -value (FDR-adj.)
	Baseline	Follow-up				
White matter lesions ^a	1462 \pm 169	1431 \pm 147	-31 [-52, -10]	2.98	0.004	0.032*
White matter lesions ^b	1462 \pm 169	1457 \pm 166	-5 [-25, 15]	0.50	0.618	0.773
Normal-appearing white matter	1074 \pm 62	1086 \pm 62	11 [-3, 26]	1.54	0.130	0.520
Cortical grey matter	1613 \pm 77	1624 \pm 68	10 [-8, 29]	1.14	0.261	0.522
Global deep grey matter	1798 \pm 93	1805 \pm 88	7 [-16, 31]	0.63	0.533	0.773
Basal ganglia	1679 \pm 94	1682 \pm 90	3 [-19, 26]	0.29	0.773	0.773
Medial temporal region	2217 \pm 109	2222 \pm 96	4 [-22, 30]	0.33	0.741	0.773
Thalami	1783 \pm 90	1798 \pm 88	15 [-9, 40]	1.23	0.225	0.522

^a Includes any voxels reclassified as lesional at 1-year follow-up

^b Only includes lesions present at baseline

Asterisk (*) indicates a significant change in T_1 over 1 year after False Detection Rate (FDR) correction

CI, confidence interval; SD, standard deviation; *uncorr.*, uncorrected for multiple comparisons

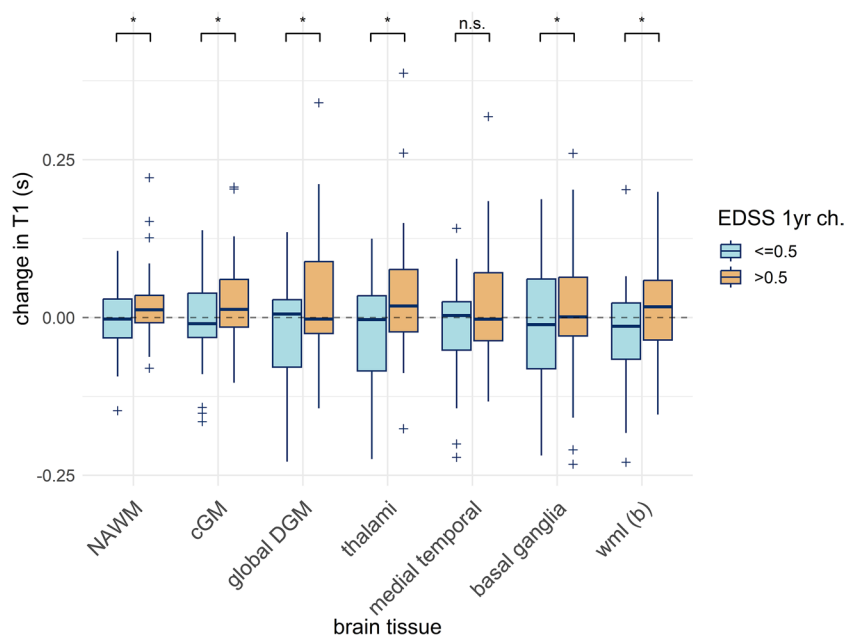


Fig. 6 One-year change in T_1 in our recently diagnosed relapsing-remitting multiple sclerosis cohort ($n=62$). Boxplots are shown for normal-appearing white matter (NAWM), cortical grey matter (cGM), global deep grey matter (DGM), thalami, medial temporal regions, basal ganglia and white matter lesions (WML, b) including only WML voxel present at baseline. Boxplots are grouped according to dichotomised change in Expanded Disability Status Scale (EDSS) score over 1 year of ≤ 0.5 and > 0.5 points. Asterisk (*) denotes significant ($p < .05$ with False Detection Rate correction) association between difference over 1 year in T_1 and disability group after adjusting for age, baseline T_1 , 1-year change in lesion load, disease-modifying therapy status and any significant interaction effects (see text for details); n.s., not significant

Table 3 Relationship between 1-year change in T_1 and change in disability in newly diagnosed relapsing-remitting multiple sclerosis ($n=62$). Results are shown for binomial logistic regression models investigating the relationship between the change in median T_1 in each tissue and dichotomised change in Expanded Disability Status Scale (EDSS) score (stable/improving vs worsening EDSS [$</\geq 0.5$ points]) over 1 year. Covariates were age, median baseline T_1 , 1-year change in white matter lesion load and disease-modifying therapy status. Continuous variables were centred and scaled, and adjusted odds ratios are for standardised data

Brain tissue	β	Adjusted odds ratio [95% CI]	Std. error	Z-value	p-value (uncorr.)	p-value (FDR-adj.)
White matter lesions ^{a,c}	1.284	3.61 [1.53, 11.00]	0.495	2.59	0.009	0.029*
White matter lesions ^{b,c}	0.998	2.71 [1.34, 6.44]	0.394	2.53	0.011	0.029*
Normal-appearing white matter	1.088	2.97 [1.35, 7.90]	0.448	2.43	0.015	0.030*
Cortical grey matter	1.236	3.44 [1.46, 9.94]	0.485	2.55	0.011	0.029*
Global deep grey matter	0.875	2.40 [1.14, 6.00]	0.417	2.10	0.036	0.041*
Basal ganglia	0.924	2.52 [1.21, 6.29]	0.416	2.22	0.026	0.035*
Medial temporal region	0.533	1.70 [0.85, 3.76]	0.372	1.44	0.151	0.151
Thalami	0.943	2.57 [1.22, 6.36]	0.417	2.26	0.024	0.035*

Asterisk (*) indicates a significant relationship at the $p < 0.05$ level after False Detection Rate (FDR) correction

^a Includes all voxels classed as white matter lesions (WML) at follow-up

^b Includes only voxels previously classed as WML at baseline

^c Mediated by a significant interaction between change in WML T_1 and age

β , standardised beta coefficient (log odds); CI, confidence interval; std., standard; uncorr., uncorrected

Table 4 Cross-sectional relationship between prolonged/supramedian T_1 white matter lesion (WML) voxel count and disability in newly diagnosed relapsing-remitting multiple sclerosis ($n=62$). Results are shown for ordinal logistic regression models investigating the relationship at (a) baseline and (b) 1-year follow-up between the number of prolonged/supramedian T_1 WML voxels and Expanded Disability Status Score (EDSS). WML voxels were classed (non-exclusively) as prolonged T_1 , where $T_1 \geq 2.00$ s, and supramedian T_1 , where $T_1 \geq$ cohort mean of baseline median WML T_1 . Covariates were age and WML load (at the respective time point)

		Number of WML voxels, mean \pm SD [range]	β	Adjusted odds ratio [95% CI]	Std. error	z-value	p-value (uncorr.)
Baseline	Prolonged T_1	691 \pm 684 ^{§§§} [20–2897]	0.822	2.27 [1.07, 4.79]	0.377	2.18	0.029*
	Supramedian T_1	1987 \pm 1846 ^{§§§} [107–7864]	1.160	3.19 [1.05, 9.47]	0.554	2.09	0.036*
One-year follow-up	Prolonged T_1	867 \pm 767 ^{§§§} [40–3166]	0.996	2.71 [1.25, 6.07]	0.393	2.53	0.011*
	Supramedian T_1	2451 \pm 2047 ^{§§§} [163–8883]	1.554	4.73 [1.56, 14.77]	0.567	2.74	0.006**

* and ** indicate significant relationship with EDSS at the $p < 0.05$ and $p < 0.01$ level, respectively

§§§ Significant change in number of prolonged/supramedian WML voxels over 1 year at $p < 0.001$ level (paired t-test)

β , standardised beta coefficient; CI, confidence interval

Longitudinal change in T_1 and prolonged WML T_1 components

We found no significant longitudinal median T_1 change in grey or white matter regions over the year following diagnosis, in line with previous serial T_1 measurements

in early RRMS [5]. A groupwise reduction in WML T_1 over time was attributable to new or enlarging WML; when only WML voxels that were present at baseline were included, no significant T_1 change was found. New WML voxels with less tissue damage developing over the

Table 5 Relationship between prolonged/supramedian T_1 white matter lesion (WML) voxel counts and 1-year change in disability in newly diagnosed relapsing-remitting multiple sclerosis ($n=62$). Results are shown for binomial logistic regression models investigating the relationship between (a) baseline and (b) 1-year change in prolonged/supramedian T_1 voxel counts and 1-year change in dichotomised Expanded Disability Status Scale (EDSS) score (stable/improving vs worsening EDSS [$</>=0.5$ point increase]). WML voxels were classed as prolonged T_1 if $T_1 \geq 2.00$ s and classed (non-exclusively) as supramedian if $T_1 \geq$ the mean average of the baseline cohort median WML T_1 . Model covariates were s age and lesion load; ss age, baseline voxel count, 1-year change in WML load and disease-modifying treatment status at follow-up (untreated versus treated)

		β	Adjusted odds ratios [95% CI]	Std. error	Z-value	p-value (uncorr.)
Baseline WML voxel count ^s	Prolonged T_1	0.097	1.10 [0.41, 3.11]	0.497	0.20	0.845
	Supramedian T_1	0.055	1.06 [0.26, 4.01]	0.674	0.08	0.935
One-year change in WML voxel count ^{ss}	Prolonged T_1^a	1.091	2.98 [1.26, 8.75]	0.482	2.26	0.024*
	Prolonged T_1^b	0.971	2.64 [1.25, 6.72]	0.42	2.33	0.020*
	Supramedian T_1^a	1.830	6.23 [1.95, 30.68]	0.687	2.67	0.008**
	Supramedian T_1^b	1.377	3.96 [1.46, 13.92]	0.566	2.43	0.015*

^a Including new lesion voxels forming over the 1-year follow-up period

^b Excluding WML forming over 1 year

Asterisks indicate significant at $p < 0.05$ (*) and $p < 0.01$ (**) levels

β , standardised beta coefficient; CI, confidence interval; *uncorr.*, uncorrected; WML, white matter lesions

follow-up period therefore appear to drive the cohort-wide WML T_1 decrease, rather than remyelination. WML T_1 reduction over time in early RRMS has been reported previously, [19] and this potential confound should be considered for future study design.

Marked intersubject variability in the proportions of higher WML T_1 components guided our focus on WML voxels with supramedian T_1 and values over 2.00 s; both aim to identify more disrupted microstructure [12]. We found that the number of thresholded T_1 WML voxels increased significantly over 1 year following RRMS diagnosis, indicating increasing microstructural damage within existing WML. To our knowledge, this study is the first to examine the longitudinal evolution of prolonged T_1 components, although thresholding approaches using T_1 [12, 22] and normalised T_1 -weighted images [35] have been applied cross-sectionally in MS.

T_1 and clinical disability

Although positive associations between clinical disability and T_1 within NAWM [14, 21] and WML [14] have been described previously, we did not find an association between cross-sectional median T_1 measures and clinical disability. Previous studies were in mixed MS subtypes at varying disease stages however, and findings varied; [40] the earlier disease stage of our more homogeneous RRMS cohort may account for these differences.

Conversely, cross-sectional prolonged T_1 and supramedian WML voxel counts were associated with EDSS score at the time of diagnosis, a relationship that persisted at 1-year follow-up. The significant increase seen in these WML components over time was also associated with EDSS worsening. This is in line with the literature, where thresholded T_1 has been shown to provide disability-relevant information additional to visual assessment of 'T₁-w hypointense' WML in more advanced disease [22]. Our data suggest that prolonged T_1 WML components contribute disproportionately to clinical disability in early RRMS, which may reflect both demyelination and axonal loss [12]. Thresholded WML T_1 measures may therefore provide useful disease stratification in early RRMS.

Longitudinal increases in median T_1 in WML tissue present at baseline in patients with worsening disability, and decreases in those with stable or improving disability, are consistent with disability-relevant microstructural damage and remyelination, respectively. An earlier study did not find any association between a derived WML load-weighted T_1 measure and 1-year change in EDSS score in RRMS, [10] which may reflect differences in cohort size, disease duration and analytical approach.

In our cohort, greater 1-year increase in median T_1 in NAWM, cGM and thalamus was also associated with EDSS worsening, whereas T_1 was relatively stable or decreasing in participants with stable or improving EDSS,

resulting in an absence of net cohort-wide T_1 change in GM or NAWM. T_1 therefore captures disability-relevant demyelination that is not visible on conventional MRI, and the direction of T_1 change over 1 year may indicate disability trajectory in early MS.

None of our baseline measures were predictive of EDSS worsening over the following year. High individual variance in baseline brain microstructural integrity, despite a relatively homogeneous diagnosis point, and limited 1-year clinical worsening following RRMS diagnosis may be limiting factors.

Limitations

T_1 quantification may be useful as a group-level patient stratifier for targeted clinical trials; the small magnitude of changes and reproducibility of measures may, however, limit application in individual patients. VFA acquisition for T_1 approximation is rapid and readily implemented, but does not correct for B_1 inhomogeneities, which may reduce sensitivity to biological change and introduce spatial bias, although unlikely to substantially effect longitudinal measures. WML were segmented on 3-mm 2D FLAIR slices rather than 3D FLAIR due to better contrast resolution, which may introduce partial volume effects. Although all participants were recruited within 6 months of diagnosis, the relationship with true disease onset is variable and difficult to determine reliably; [41] diagnosis was therefore chosen as a pragmatic and measurable time point. Effects of intercurrent treatment are likely to be minimal: MRI was performed a minimum of 3 weeks post-steroid treatment; DMT status was not related to disability outcome; however, treatment variation in this cohort precludes meaningful sensitivity analysis. Innate EDSS limitations are well-recognised [42]. Moreover, 1-year change in EDSS score showed significant intersubject variability (Fig. S3); overall disability worsening was minor, and confounded by improvement following the clinical episode that initiated RRMS diagnosis. Five-year follow-up of the FutureMS cohort [23] will allow more reliable evaluation of T_1 measures as predictors of disease trajectory.

Conclusion

Quantitative T_1 mapping is sensitive to disability-relevant microstructural changes in the year following RRMS diagnosis. T_1 thresholding approaches demonstrate heterogeneity of microstructural damage in WML; WML components with prolonged T_1 increase with time, and are significantly associated with clinical disability. Widespread subtle demyelination can also be detected in NAWM and GM in patients with worsening disability. Further studies in well-characterised RRMS cohorts over longer time periods will help clarify the utility of T_1 mapping as a disease stratifier, and for potential application in future therapeutic trials.

Abbreviations

cGM	Cortical grey matter
DGM	Deep grey matter
DMTs	Disease-modifying therapies
EDSS	Expanded Disability Status Scale
FDR	False discovery rate
FLAIR	Fluid-attenuated inversion recovery
GM	Grey matter
MRI	Magnetic resonance imaging
NAWM	Normal-appearing white matter
RRMS	Relapsing-remitting multiple sclerosis
T_1	Spin-lattice relaxation time
VFA	Variable flip angle
WML	White matter lesions

Supplementary Information

The online version contains supplementary material available at <https://doi.org/10.1007/s00330-023-10351-6>.

Below is the link to the electronic supplementary material. Supplementary file1 (PDF 661 KB)

Acknowledgements

With special thanks to all participants in FutureMS and the radiographers at the RIE Edinburgh. We would also like to thank other non-author contributors of the FutureMS consortium. For the purpose of open access, the author has applied a Creative Commons Attribution (CC BY) licence to any Author Accepted Manuscript version arising from this submission.

Collaborators: on behalf of the FutureMS consortium

Amit Akula, Sergio Baranzini, Fiona Barret, Mark Bastin, Chris Batchelor, Emily Beswick, Fraser Brown, Tracy Brunton, Javier Carod Artal, Jessie Chang, Yingdi Chen, Shuna Colville, Peter Connick, Annette Cooper, Denise Cranley, Rachel Dakin, Baljean Dhillon, Liz Elliott, James Finlayson, Peter Foley, Stella Glas-macher, Angus Grossart, Haane Haagenrud, Katarzyna Hafezi, Emily Harrison, Adil Harroud, Sara Hathorn, Tracey Hopkins, David Hunt, Aidan Hutchison, Charlotte Jardine, Kiran Jayprakash, Matt Justin, Gwen Kennedy, Lucy Kessler, Michaela Kleynhans, Juan Larraz, Katherine Love, Dawn Lyle, James MacDon-ald, Niall MacDougall, Jen MacFarlane, Lesley Macfarlane, Alan Maclean, Bev MacLennan, Margaret-Ann MacLeod, Nicola Macleod, Don Mahad, Sarah-Jane Martin, Conni McCarthy, Lynn McMahon, Daisy Mollison, Ian Megson, Daisy Mollison, Mary Monaghan, Lee Murphy, Katy Murray, Judith Newton, Julian Ng Kee Kwong, Jonathan O'Riordan, David Perry, Suzanne Quigley, Adam Scotson, Scott Semple, Amy Stenson, Michaela Stuart, Christine Weaver, Stuart Webb, Belinda Weller, Nicole White, Anna Williams, Stewart Wiseman, Charis Wong, Michael Wong and Rosie Woodward.

Funding

ENY was supported by a Chief Scientist Office SPRINT MND/MS Studentship (MMPP/01) and funding from the Anne Rowling Regenerative Neurology Clinic, University of Edinburgh. MJT is funded by the NHS Lothian Research and Development Office. RM and AK are funded by the UK MS Society Edinburgh Centre for MS Research grant (grant reference 133). PKAK is supported by an ECAT-Wellcome fellowship (223058/Z/21/Z). MVH is supported by the Row Fogo Charitable Trust (BRO-D.FID3668413). FutureMS, hosted by Precision Medicine Scotland Innovation Centre (PMS-IC), was funded by a grant from the Scottish Funding Council to PMS-IC and Biogen Idec Ltd. Insurance. The study E161616 FutureMS was undertaken at the Edinburgh Imaging facility RIE (Royal Infirmary of Edinburgh), University of Edinburgh. Additional funding for the University of Edinburgh 3 T MRI Research scanner in Royal Infirmary Edinburgh is provided by Wellcome (104916/Z/14/Z), Dunhill Trust (R380R/1114), Edinburgh and Lothians Health Foundation (2012/17), Muir Maxwell Research Fund, Edinburgh Imaging and University of Edinburgh. This work is supported by the UK Dementia Research Institute which receives its funding from UK DRI Ltd., funded by the UK Medical Research Council, Alzheimer's Society and Alzheimer's Research UK.

Data availability

Researchers may request access to anonymised patient data from FutureMS-1 following our standard procedures. To submit an access, request please contact future-ms@ed.ac.uk. Proposals will be reviewed and approved by the FutureMS steering committee. A signed data sharing agreement will then be issued. Data will be available as soon as possible after the first publication of the results.

Declarations

Guarantor

The scientific guarantor of this publication is Professor Adam Waldman.

Conflict of interest

The authors of this manuscript declare no relationships with any companies, whose products or services may be related to the subject matter of the article.

Statistics and biometry

One of the authors has significant statistical expertise.

Informed consent

Written informed consent was obtained from all subjects in this study.

Ethical approval

Institutional Review Board approval was obtained (South East Scotland Research Ethics Committee 02).

Study subjects or cohorts overlap

The current article focuses on quantitative T_1 data from a sub-cohort of FutureMS participants who received extended microstructural MRI, and test-retest healthy control T_1 data, which have not been reported on previously. FutureMS studies which have been previously published:

1. Glasmacher SA, Kearns PKA, Hassan Z, et al (2022) The influence of disease-modifying therapy on hidden disability burden in people with newly diagnosed relapsing-remitting multiple sclerosis. *Multiple Sclerosis and Related Disorders*. <https://doi.org/10.1016/j.msard.2022.103837>.
2. Chang Y-T, Kearns PKA, Carson A, et al (2023) Network analysis characterizes key associations between subjective fatigue and specific depressive symptoms in early relapsing-remitting multiple sclerosis. *Multiple Sclerosis and Related Disorders*. <https://doi.org/10.1016/j.msard.2022.104429>.
3. Kearns PKA, Martin SJ, Chang J, et al (2022) FutureMS cohort profile: a Scottish multicentre inception cohort study of relapsing-remitting multiple sclerosis. *BMJ Open*. <https://doi.org/10.1136/bmjopen-2021-058506>.
4. York EN, Meijboom R, Thrippleton MJ, et al (2022) Longitudinal microstructural MRI markers of demyelination and neurodegeneration in early relapsing-remitting multiple sclerosis: magnetisation transfer, water diffusion and g-ratio. *Neuroimage: Clinical*. <https://doi.org/10.1016/j.nicl.2022.103228>.
5. York EN, Martin SJ, Meijboom R, et al (2021) MRI-derived g-ratio and lesion severity in newly diagnosed multiple sclerosis. *Brain Commun*. <https://doi.org/10.1093/braincomms/fcab249>.
6. Ng Kee Kwong KC, Mollison D, Meijboom R, et al (2022) Rim lesions are demonstrated in early relapsing-remitting multiple sclerosis using 3 T-based susceptibility-weighted imaging in a multi-institutional setting. *Neuroradiology*. <https://doi.org/10.1007/s00234-021-02768-x>.
7. Chen Y, Larraz J, Wong M, et al (2022) Longitudinal retinal imaging study of newly diagnosed relapsing-remitting multiple sclerosis in Scottish population: baseline and 12 months follow-up profile of FutureMS retinal imaging cohort. *BMJ Open Ophthalmology*. <https://doi.org/10.1136/bmjophth-2022-001024>.
8. Meijboom R, York EN, Kampaita A, et al Patterns of brain atrophy in recently-diagnosed relapsing-remitting multiple sclerosis. *PLoS One*. 2023;18(7):e0288967. Published 2023 Jul 28. <https://doi.org/10.1371/journal.pone.0288967>

Methodology

- prospective
- observational
- performed at one institution

Author details

¹Centre for Clinical Brain Sciences, University of Edinburgh, Edinburgh BioQuarter: Chancellors Building, Edinburgh EH16 4SB, UK. ²Edinburgh Imaging, University of Edinburgh, Edinburgh, UK. ³Anne Rowling Regenerative Neurology Clinic, Edinburgh, UK. ⁴UK Dementia Research Institute, University of Edinburgh, Edinburgh, UK.

Received: 29 March 2023 Revised: 20 July 2023

Accepted: 29 August 2023 Published online: 9 November 2023

References

1. Chaudhuri A (2013) Multiple sclerosis is primarily a neurodegenerative disease. *J Neural Transm*. <https://doi.org/10.1007/s00702-013-1080-3>
2. Thompson AJ, Banwell BL, Barkhof F et al (2018) Diagnosis of multiple sclerosis: 2017 revisions of the McDonald criteria. *Lancet Neurol*. [https://doi.org/10.1016/s1474-4422\(17\)30470-2](https://doi.org/10.1016/s1474-4422(17)30470-2)
3. Barkhof F (1999) MRI in multiple sclerosis: correlation with expanded disability status scale (EDSS). *Mult Scler J*. <https://doi.org/10.1177/135245859900500415>
4. Chard D, Trip SA (2017) Resolving the clinico-radiological paradox in multiple sclerosis [version 1; peer review: 3 approved]. *F1000Res*. <https://doi.org/10.12688/f1000research.11932.1>
5. Davies GR, Hadjiprocopis A, Altmann DR et al (2007) Normal-appearing grey and white matter T_1 abnormality in early relapsing-remitting multiple sclerosis: a longitudinal study. *Mult Scler J*. <https://doi.org/10.1177/1352458506070726>
6. Absinta M, Sati P, Gaitán MI et al (2013) Seven-tesla phase imaging of acute multiple sclerosis lesions: a new window into the inflammatory process. *Ann Neurol*. <https://doi.org/10.1002/ana.23959>
7. Harrison DM, Li X, Liu H et al (2016) Lesion heterogeneity on high-field susceptibility MRI is associated with multiple sclerosis severity. *AJNR Am J Neuroradiol*. <https://doi.org/10.3174/ajnr.A4726>
8. Yao B, Bagnato F, Matsuura E et al (2012) Chronic multiple sclerosis lesions: characterization with high-field-strength MR imaging. *Radiology*. <https://doi.org/10.1148/radiol.11110601>
9. York EN, Martin SJ, Meijboom R et al (2021) MRI-derived g-ratio and lesion severity in newly diagnosed multiple sclerosis. *Brain Commun*. <https://doi.org/10.1093/braincomms/fcab249>
10. Thaler C, Faizy TD, Sedlacik J et al (2017) T1 recovery is predominantly found in black holes and is associated with clinical improvement in patients with multiple sclerosis. *AJNR Am J Neuroradiol*. <https://doi.org/10.3174/ajnr.A5004>
11. Gowland PA, Stevenson VL (2003) T1: the longitudinal relaxation time. In: Tofts PS (ed) *Quantitative MRI of the brain: measuring changes caused by disease*. Chichester, West Sussex; Hoboken, N.J.: Wiley, pp 111–141
12. Kolb H, Absinta M, Beck ES et al (2021) 7T MRI differentiates remyelinated from demyelinated multiple sclerosis lesions. *Ann Neurol*. <https://doi.org/10.1002/ana.26194>
13. Truyen L, van Waesberghe JH, van Walderveen MAA et al (1996) Accumulation of hypointense lesions ("black holes") on T_1 spin-echo MRI correlates with disease progression in multiple sclerosis. *Neurology*. <https://doi.org/10.1212/wnl.47.6.1469>
14. Parry A, Clare S, Jenkinson M, Smith S, Palace J, Matthews PM (2002) White matter and lesion T1 relaxation times increase in parallel and correlate with disability in multiple sclerosis. *J Neurol*. <https://doi.org/10.1007/s00415-002-0837-7>
15. Griffin CM, Chard DT, Parker GJM, Barker GJ, Thompson AJ, Miller DH (2002) The relationship between lesion and normal appearing brain tissue abnormalities in early relapsing remitting multiple sclerosis. *J Neurol*. <https://doi.org/10.1007/PL00007864>
16. Niepel G, Tench CR, Morgan PS, Evangelou N, Auer DP, Constantinescu CS (2006) Deep gray matter and fatigue in MS: a T1 relaxation time study. *J Neurol*. <https://doi.org/10.1007/s00415-006-0128-9>
17. Steenwijk MD, Vrenken H, Jonkman LE et al (2016) High-resolution T1-relaxation time mapping displays subtle, clinically relevant, gray matter damage in long-standing multiple sclerosis. *Mult Scler J*. <https://doi.org/10.1177/1352458515615953>

18. Lommers E, Simon J, Reuter G et al (2019) Multiparameter MRI quantification of microstructural tissue alterations in multiple sclerosis. *Neuroimage Clin.* <https://doi.org/10.1016/j.nicl.2019.101879>
19. Bonnier G, Maréchal B, Fartaria MJ et al (2017) The combined quantification and interpretation of multiple quantitative magnetic resonance imaging metrics enlightens longitudinal changes compatible with brain repair in relapsing-remitting multiple sclerosis patients. *Front Neurol.* <https://doi.org/10.3389/fneur.2017.00506>
20. Al-Radaideh A, Athamneh I, Alabadi H, Hbabbih M (2020) Deep gray matter changes in relapsing-remitting multiple sclerosis detected by multi-parametric, high-resolution magnetic resonance imaging (MRI). *Eur Radiol.* <https://doi.org/10.1007/s00330-020-07199-5>
21. West J, Aalto A, Tisell A et al (2014) Normal appearing and diffusely abnormal white matter in patients with multiple sclerosis assessed with quantitative MR. *PLoS One.* <https://doi.org/10.1371/journal.pone.0095161>
22. Thaler C, Faizy T, Sedlacik J et al (2015) T1- thresholds in black holes increase clinical-radiological correlation in multiple sclerosis patients. *PLoS One.* <https://doi.org/10.1371/journal.pone.0144693>
23. Kearns PKA, Martin SJ, Chang J et al (2022) FutureMS cohort profile: a Scottish multicentre inception cohort study of relapsing-remitting multiple sclerosis. *BMJ Open.* <https://doi.org/10.1136/bmjopen-2021-058506>
24. Meijboom R, Wiseman SJ, York EN et al (2022) Rationale and design of the brain magnetic resonance imaging protocol for FutureMS: a longitudinal multi-centre study of newly diagnosed patients with relapsing-remitting multiple sclerosis in Scotland. *Wellcome Open Res.* <https://doi.org/10.12688/wellcomeopenres.17731.1>
25. Zhan T, Zhan Y, Liu Z, Xiao L, Wei Z (2015) Automatic method for white matter lesion segmentation based on T1-fluid-attenuated inversion recovery images. *IET Comput Vis.* <https://doi.org/10.1049/iet-cvi.2014.0121>
26. Helms G, Dathe H, Dechent P (2008) Quantitative FLASH MRI at 3T using a rational approximation of the Ernst equation. *Magn Reson Med.* <https://doi.org/10.1002/mrm.21542>
27. York EN, Thrippleton MJ, Waldman A (2020) Magnetisation transfer saturation (MTsat) processing, [software]. University of Edinburgh. Centre for Clinical Brain Sciences. <https://doi.org/10.7488/ds/2965>
28. Jenkinson M, Bannister P, Brady M, Smith S (2002) Improved optimization for the robust and accurate linear registration and motion correction of brain images. *Neuroimage.* [https://doi.org/10.1016/s1053-8119\(02\)91132-8](https://doi.org/10.1016/s1053-8119(02)91132-8)
29. York EN, Meijboom R, Thrippleton MJ et al (2022) Longitudinal microstructural MRI markers of demyelination and neurodegeneration in early relapsing-remitting multiple sclerosis: Magnetisation transfer, water diffusion and g-ratio. *Neuroimage Clin.* <https://doi.org/10.1016/j.nicl.2022.103228>
30. Benjamini Y, Hochberg Y (1995) Controlling the false discovery rate: a practical and powerful approach to multiple testing. *J R Stat Soc B.* <https://doi.org/10.1111/j.2517-6161.1995.tb02031.x>
31. Schmierer K, Scaravilli F, Altmann DR, Barker GJ, Miller DH (2004) Magnetization transfer ratio and myelin in postmortem multiple sclerosis brain. *Ann Neurol.* <https://doi.org/10.1002/ana.20202>
32. Fatouros PP, Marmarou A, Kraft KA, Inao S, Schwarz FP (1991) *In vivo* brain water determination by T_1 measurements: effect of total water content, hydration fraction, and field strength. *Magn Reson Med.* <https://doi.org/10.1002/mrm.1910170212>
33. MacDonald HL, Bell BA, Smith MA et al (1986) Correlation of human NMR T_1 values measured *in vivo* and brain water content. *Br J Radiol.* <https://doi.org/10.1259/0007-1285-59-700-355>
34. van Walderveen MAA, Kamphorst W, Scheltens P et al (1998) Histopathologic correlate of hypointense lesions on T1-weighted spin-echo MRI in multiple sclerosis. *Neurology.* <https://doi.org/10.1212/wnl.50.5.1282>
35. Naval-Baudin P, Pons-Escoda A, Camins A et al (2023) Deeply 3D-T1-TFE hypointense voxels are characteristic of phase-rim lesions in multiple sclerosis. *Eur Radiol.* <https://doi.org/10.1007/s00330-023-09784-w>
36. Griffin CM, Dehmeshki J, Chard DT et al (2002) T1 histograms of normal-appearing brain tissue are abnormal in early relapsing-remitting multiple sclerosis. *Mult Scler J.* <https://doi.org/10.1191/1352458502ms807oa>
37. Ormerod IEC, Miller, DH, McDonald WI (1987) The role of NMR imaging in the assessment of multiple sclerosis and isolated neurological lesions: a quantitative study. *Brain.* <https://doi.org/10.1093/brain/110.6.1579>
38. Larsson HB, Frederiksen J, Kjaer L, Henriksen O, Olesen J (1988) *In vivo* determination of T1 and T2 in the brain of patients with severe but stable multiple sclerosis. *Magn Reson Med.* <https://doi.org/10.1002/mrm.1910070106>
39. Stevenson VL, Parker GJM, Barker GJ et al (2000) Variations in T1 and T2 relaxation times of normal appearing white matter and lesions in multiple sclerosis. *J Neurol Sci.* [https://doi.org/10.1016/s0022-510x\(00\)00339-7](https://doi.org/10.1016/s0022-510x(00)00339-7)
40. Pontillo G, Petracca M, Monti S et al (2023) Clinical correlates of R1 relaxometry and magnetic susceptibility changes in multiple sclerosis: a multi-parameter quantitative MRI study of brain iron and myelin. *Eur Radiol.* <https://doi.org/10.1007/s00330-022-09154-y>
41. Kaufmann M, Kuhle J, Puhon MA et al (2018) Factors associated with time from first-symptoms to diagnosis and treatment initiation of Multiple Sclerosis in Switzerland. *Mult Scler J Exp Transl Clin.* <https://doi.org/10.1177/2055217318814562>
42. van Munster CEP, Uitdehaag BMJ (2017) Outcome measures in clinical trials for multiple sclerosis. *CNS Drugs.* <https://doi.org/10.1007/s40263-017-0412-5>

Publisher's Note

Springer Nature remains neutral with regard to jurisdictional claims in published maps and institutional affiliations.